17. Utsumi, A., Matsuda, J., Yoneda, M., Katsumura, M. (2002). Effect of base metal travelling direction on TIG arc behaviour. Study of high-speed surface treatment by combined use of laser and arc welding (Report 4). Welding International, 16 (7), 530–536. doi: https://doi.org/10.1080/09507110209549571
18. Cho, W.-I., Na, S.-J. (2007). A Study on the Process of Hybrid Welding Using Pulsed Nd:YAG Laser and Dip-transfer DC GMA Heat Sources. Journal of Welding and Joining, 25 (6), 71–77. doi: https://doi.org/10.5781/kwjs.2007.25.6.071
19. Goldak, J. A., Akhlaghi, M. (2005). Computational welding mechanics. Boston. doi: https://doi.org/10.1007/b101137
20. Bofang, Z. (2018). The Finite Element Method: Fundamentals and Applications in Civil, Hydraulic, Mechanical and Aeronautical Engineering. John Wiley & Sons Singapore Pte. Ltd. doi: https://doi.org/10.1002/9781119107323

Досліджено можливості використання енергетичного методу для розрахунку енергосилових параметрів процесів холодного видавлювання деталей складної конфігурації. Запропоновано математичну модель процесу комбінованого послідовного радіально-прямого видавлювання з обтисненням з наявністю трикутних кінематичних модулів. Використання кінематичних модулів трикутної форми з криволінійними та прямолінійними межами дозволило описати осередки інтенсивної деформації, що відповідають сталій стадії процесу деформування. Запропоновано використовувати верхню оцінку потужності сил деформування кінематичного модуля трикутної форми зони переходи від радіальної течії металу до прямого видавлювання. Це дозволило отримати величину приведеного тиску деформування в аналітичному вигляді як функцію від геометричних та технологічних параметрів процесу видавлювання. Похибка у порівнянні із чисельними розрахунками без застосування верхньої оцінки не перевищує 0,2–1 %. Роль параметру оптимізації відіграє $a \in (0,1)$, що відповідає за форму криволінійної границі внутрішнього трикутного кінематичного модуля. Отримано аналітичний вираз оптимального значення параметра α та проаналізовано змінення величини приведеного тиску деформування за різних співвідношень геометричних параметрів процесу. Встановлено, що оптимальне значення кута нахилу твірної оправлення β знаходиться в межах від 20° до 30° для різних співвідношень процесу деформування.

Обґрунтовано, що використання комбінованого послідовного видавлювання при виготовленні порожнистих деталей з фланцем, у порівнянні з використанням простих схем деформування, підвищує технологічні можливості процесу. Підтверджено недостатню вивченість схем процесу комбінованого радіально-прямого видавлювання з обтисненням деталей типу втулка та брак рекомендацій щодо розрахунку енергосилових параметрів процесу. Розроблена на основі енергетичного методу розрахункова схема даного процесу дозволяє прогнозувати силовий режим для сталої стадії для різних технологічних параметрів процесу деформування. Отримані дані щодо оцінки оптимальних параметрів конфігурації інструменту сприятиме розробці відповідних конструкторсько-технологічних рекомендацій

Ключові слова: комбіноване видавлювання, верхня оцінка, кінематичний модуль, енергетичний метод, процес деформування, деталі з фланцем

UDC 621.777.01
DOI: 10.15587/1729-4061.2020.198433

EFFECT OF THE TOOL GEOMETRY ON THE FORCE MODE OF THE COMBINED RADIAL-DIRECT EXTRUSION WITH COMPRESSION

L. Aliieva
Doctor of Technical Sciences,
Associate Professor*
N. Hrudkina
PhD*
E-mail: vm.grudkina@ukr.net
I. Aliiev
Doctor of Technical Sciences,
Professor, Head of Department*
I. Zhbankov
Doctor of Technical Sciences,
Associate Professor*
O. Markov
Doctor of Technical Sciences,
Professor, Head of Department
Department of Computerized Design and Modeling of Processes and Machines**
*Department of Metal Forming**
**Donbass State Engineering Academy
Akademichna str., 72,
Kramatorsk, Ukraine, 84313

Received date 17.01.2020
Accepted date 04.03.2020
Published date 27.04.2020

1. Introduction

Cold extrusion processes provide high surface quality and precise sizes of stamped blanks and components. This, in turn, reduces or eliminates the need for additional machining by cutting [1, 2]. The most common conventional extrusion techniques are the longitudinal (inverse and direct) extrusion methods, which are characterized by the flow of the

extruded metal along the longitudinal axis of symmetry [3]. The components that are complex in shape should be made by using the techniques of transverse (radial and lateral) and combined transverse-longitudinal extrusion [2]. In this case, stamps with matrixes are used, whose transverse (circular or channel) receiving cavity is made detachable, mainly on a horizontal (transverse) plane [4].

Combining the longitudinal and transverse extrusion schemes is necessary to create more complex deformation techniques. This makes it possible to fabricate, in a single run, solid and hollow components with flanges or rames, with deep cavities. or other configurations. Depending on the nature of the combination of simple transverse and longitudinal extrusion schemes in a single combined process, the techniques are divided into combined and consistent, over time or along the path of deformation, extrusion techniques. The combined techniques are characterized by the presence of one common site or adjacent deformation sites and several possible directions for a blank's metal outflow. The use of a combination of simple deformation schemes is mainly aimed at optimizing the strength regime to improve the resilience of the tool and the stability of a cold deformation process [1, 4]. A series of combined extrusion techniques aim to enhance the capabilities of punching technologies by complicating the shape of the components and providing the required specifications of parts [5].

2. Literature review and problem statement

Our analysis of publications is preceded by a generalization of the techniques for consistent radial-longitudinal extrusion, designed to obtain hollow components. There are two main types of these techniques: the extrusion schemes with the expansion of metal (Table 1, row A) [5–9] and the extrusion schemes with the compression of metal at its radial flow (Table 1, row B) [5, 10–12].

Group A extrusion schemes are distinguished by the consistent execution of radial and longitudinal extrusion operations. In this case, the radial extrusion of the metal occurs with the expansion, that is, by the flow of the metal from the center of a blank to the periphery. When the «matrix-free extrusion» techniques are employed, the metal is extruded simultaneously through the lateral and lower end of the blank (A1) or through the side surface of the blank (A2) [5, 6]. These techniques are applied to make deep hollow vessels, which significantly reduces the force of deformation compared to the use of reverse extrusion [4, 7]. The extrusion techniques to fabricate components from a solid blank as a result of the developed radial current, which is replaced by a straight (A3 scheme) or reverse current of the deformed metal (A4 scheme), are used, respectively, for the manufacture of deep casings [5, 7] and cups [8, 9]. The process of deformation in line with the scheme of radial-direct extrusion with expansion makes it possible to reduce the forces of deformation by reducing the area of contact between an active deforming tool and a blank. However, this is accompanied by a marked increase in the specific loads on the tool, which limits the possibilities of the process.

The radial-direct extrusion techniques from group B differ in that they imply the radial extrusion of metal in the direction from the periphery to the center. That is why they are termed the techniques of consistent radial-direct extrusion with compression [5, 10–12]. Depending on the tool used, the way the metal is fed at the direct current stage and, accordingly, the outflow degree of freedom, several extrusion schemes are distinguished (B1 and B2 schemes). The B3 scheme is characterized by the use of a conical mandrel capable of recurrent movement, which is necessary to obtain components with variable wall thickness [10]. When profiling a mandrel (B4 scheme), it is possible to make components with the ribbed inner surface. Subject to providing the mandrel with an independent drive for longitudinal movement and turning around the axis, one could get components with a profiled inner surface [10, 11] or with many spiral grooves on the inner wall [12].

Table 1

Schemes of combined sequential radial-straight extrusion with expansion (row A) and compression (row B)

	1	2	3	4
A	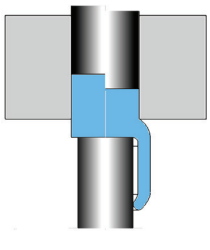	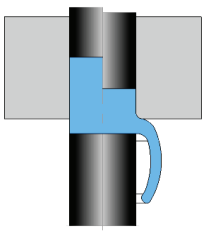	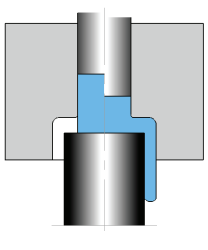	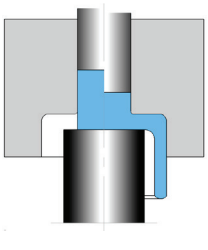
B	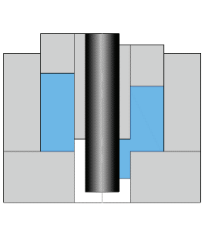	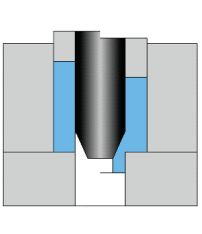	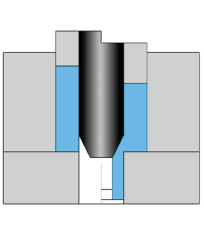	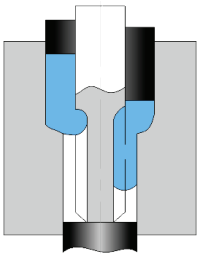

In recent years, many researchers have shown interest in the processes of combined radial-longitudinal extrusion. Analysis of force and deformation regimes of these processes is performed mainly experimentally, by applying methods of finite elements (FEM) and upper estimate. Work [7] investigated the impact of some important structural geometric parameters of the process of sequential radial-direct extrusion (the flange thickness, the size of the ring gap, the mandrel radius) on the emergence and fluctuations of the load. However, the conclusion that the counterpunch radius and the curvature radii of the tool's transition sections have little impact on the formation of the load on the punch and the counter punch is questionable. Paper [13] describes the strength characteristics of the process of

sequential radial-longitudinal extrusion. The authors used the experiment and a finite element model to show the effect of such design parameters as the mandrel diameter, the radius of the matrix, and the friction conditions, on the forces of deformation, but they failed to give a quantitative description of these dependences.

As shown in study [14], the radial-direct extrusion is also an effective method for the production of articles such as large-diameter pipes from small cylindrical blanks. The flow of material along the radial and direct channels causes large deformations and, therefore, results in the improved mechanical and metallurgical properties of the product. With the use of additional hydrostatic pressure at the deformation site and the introduction of the sign-alternating character of deformation, there is a significant increase in strength along with a very low loss of plasticity and high homogeneity of a part's rigidity indicators. However, the issues related to the calculation of increased energy costs and loads on the tool remained unresolved.

A series of papers address the assessment of the stressed-strained state of the blank and tool, the wear and condition of the surface of the tool, the conditions for the emergence of defects of components and the deformity of metallic blanks during cold combined extrusion [15–17]. Work [15] assessed the stressed-strained state (SSS) and the limit of shape change in blanks made from various materials in the processes of cold volumetric deformation based on the combined schemes. The cited work calculates the plasticity resource according to various criteria for the process of combined radial-direct extrusion. The main purpose of studies [16, 17] that use a finite element method to investigate the radial-longitudinal extrusion process is to examine the effect of the tool geometry on the SSS characteristics of hollow articles and the tool wear. A common limitation of the results of these studies is the lack of calculated dependences to describe the effect exerted on the force mode of cold deformation by the process conditions and parameters.

To derive the estimated dependences of force and deformation parameters for the processes of cold combined extrusion of hollow components, studies [10, 18, 19] were conducted employing theoretical analysis methods. Work [18] analyzes the force parameters and the shape formation of components in the process of radial-longitudinal extrusion. The authors considered a possibility of predicting the process of defect formation, the type of a shrinkage cavity, by the method of upper estimate (rigid kinematic elements) under a flat-deformed state of the blank. Paper [10] reports an analysis of the force mode of the process of sequential radial-direct extrusion with the compression of a hollow part, the type of a sleeve. The upper estimate method was used to examine the effect of the process geometric parameters, such as the mandrel angle, the size of the overlap, and the width of the direct flow gap, as well as the friction conditions. The upper estimate method for the total load of the process was applied to investigate the technique of combined radial-direct extrusion of pipes [19]. The constructed models make it possible to determine the force mode of deformation very approximately, as the accepted assumption about the flat-deformed state of the extruded sample is quite rough.

To overcome these limitations, a series of works apply an analytical approach based on the identification of the kinematically possible velocity fields (KPVF) of the axisymmetric current in line with the energy capacity balance method [22, 23].

A model of the process using the simplest velocity fields of parallel current was proposed in [20] for the axisymmetric process of the radial-direct extrusion of components, the type of casings. Similarly, by using the energy method, the process of the combined extrusion of a hollow part from an aluminum alloy was examined in [21] in order to establish the characteristics of energy consumption. The energy method helped establish a share of significant costs to overcome the forces of contact friction in the total energy of shape formation of hollow components in the process of cold extrusion. However, these solutions that employ the parallel current KPVF, that is, the kinematic modules (zones) of rectangular shape, which could not describe the deformation site of complex configuration, are also approximate in character.

Hollow components of the type of a sleeve are widespread in the industry and it is a relevant task to derive the estimation dependences in order to design the processes of their extrusion. This is due to the fact that, along with the above benefits of the combined processes, there are a series of challenges associated with the complex stressed-strained state of a blank under conditions of extreme loads and the nature of metal outflow [5, 10]. In this case, the focus should be on the development of refined mathematical models for the calculation of technological modes, and first of all, the force parameters at the combined flow of metal with compression, which is characterized by the increased hydrostatic pressure in a plastic zone. At the same time, the complexity of the tool geometry emphasizes the task of calculating the reduced pressure of the new kinematic modules of trapezoidal and triangular shapes with different types of borders.

Our analysis of literary data reveals that the main issue holding back the application of combined extrusion processes in the industry is the lack of recommendations for calculating and developing the technology and designing the tool.

3. The aim and objectives of the study

The aim of this study is to identify patterns of the course, as well as construct mathematical models for the calculation, of the energy-force modes of combined radial-direct extrusion with the compression of components such as sleeves on the conical mandrel.

To accomplish the aim, the following tasks have been set:

– to devise an estimation scheme of the combined radial-direct extrusion process with compression using modules with a non-parallel flow;

– to investigate the effect of the tool geometry on the force mode of the combined radial-direct extrusion process with compression;

– to conduct a comparative analysis of the force parameters of the extrusion process, obtained theoretically on the basis of the constructed mathematical model, with experimentally acquired data.

4. Theoretical analysis of the process of combined radial-direct extrusion with compression

4. 1. Development of an estimation scheme for the combined radial-direct extrusion process with compression

The effective theoretical methods of calculating cold combined extrusion processes include the energy method [22–24]. To calculate the axisymmetric processes, the deformed volume

of a blank is split into axisymmetric kinematic modules with the corresponding kinematically possible velocity fields (KPVF). In this case, the complexity of the shape of the profiled blanks requires the development of new kinematic modules of trapezoidal and triangular shape. The calculation of the power of plastic deformation forces inside a kinematic module, the cutting forces with the adjoining modules, and the friction forces at the surface of the tool was considered in works [25–27]. It has been established that it is difficult to obtain an analytical expression of the power of the forces of deformation and impossible to use the linearization of deformation rates. It has been proposed to apply the upper estimate of the deformation forces power by Cauchy-Bunyakovsky or cubature formulae [26, 27]. Such calculations are required by the triangular modules with a sloping curved or straight-line boundary or the curvilinear modules of different configurations.

Consider the estimation scheme of the process of combined radial-direct extrusion with compression, including triangular kinematic modules 2 and 3 with curvilinear and straight-line borders, respectively. and rigid modules 1 and 4.

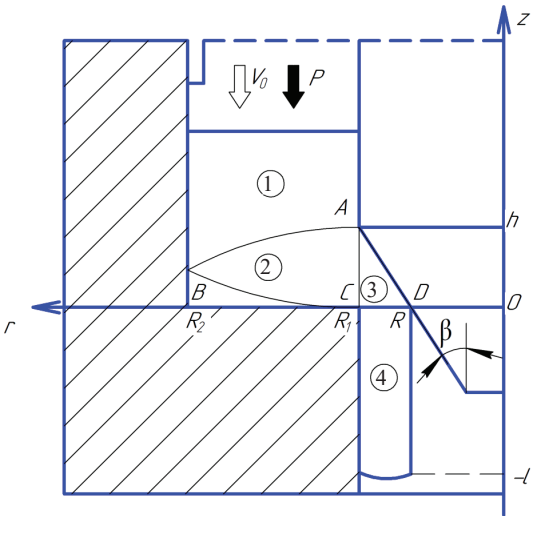

Fig. 1. Estimation scheme of the process of combined radial-direct extrusion with compression

The KPVF of rigid modules 1 and 4 takes the form:

$$\begin{cases} V_{z_1} = -V_0; \\ V_{r_2} = 0. \end{cases} \quad (1)$$

$$\begin{cases} V_{z_4} = -2\dfrac{C}{\mathrm{tg}\beta}V_0; \\ V_{r_4} = 0. \end{cases} \quad (2)$$

where

$$C = \frac{R_2^2 - R_1^2}{2h(R_1 + R)}, \quad \mathrm{tg}\beta = \frac{R_1 - R}{h}.$$

For modules of plastic deformation 2 and 3, the KPVF, the equations of curvilinear and sloping boundaries, the expression of the intensity of deformation rates $\dot{\varepsilon}_i$ are given in Table 2.

The calculations of the power of the forces of deformation, the cutting and friction forces for kinematic modules 1, 2, and 4, are known and do not cause difficulties when fitting to the new estimation schemes.

Table 2

Equations of curvilinear boundaries and KPVF of plastic deformation modules

No.	KPVF	Curvilinear boundary equations, expression of deformation rate intensity $\dot{\varepsilon}_i$
2	$\begin{cases} V_{z_2} = -\alpha V_0; \\ V_{r_2} = -\dfrac{R_2^2 - R_1^2}{2hr}V_0 \end{cases}$	$Z_{AB} = \left(\dfrac{(1-\alpha)(r^2 - R_1^2)}{R_1^2 - R_2^2} + 1\right)h;$ $Z_{BC} = \dfrac{\alpha(r^2 - R_1^2)}{R_1^2 - R_2^2}h;$ $\dot{\varepsilon}_i = \dfrac{R_2^2 - R_1^2}{\sqrt{3}hr^2}V_0$
3	$\begin{cases} V_{z_3} = -\dfrac{2C}{\mathrm{tg}\beta}\left(1 - \dfrac{\mathrm{tg}\beta}{2r}z\right)V_0; \\ V_{r_3} = -C\left(1 + \dfrac{R}{r}\right)V_0, \end{cases}$ where $C = \dfrac{R_2^2 - R_1^2}{2h(R_1 + R)}$.	$Z_{AD} = \dfrac{1}{\mathrm{tg}\beta}(r - R),$ where $\mathrm{tg}\beta = \dfrac{R_1 - R}{h};$ $\dot{\varepsilon}_i = \dfrac{C}{\sqrt{3r^2}}V_0\sqrt{4(r^2 + Rr + R^2) + z^2}$

The power of deformation, cutting, and friction forces for kinematic module 3 was obtained in the analytical form:

$$Nc_{2-3} = \frac{2\pi\sigma_s}{\sqrt{3}}V_0\left|\frac{(R_2^2 - R_1^2)(3R_1 + R)}{4R_1(R_1^2 - R^2)} - \alpha\right|. \quad (3)$$

$$Nc_{3-4} = \frac{2\pi\sigma_s}{\sqrt{3}}V_0\left[\frac{R_1^2 - R^2}{2} + R(R_1 - R)\right]\frac{R_2^2 - R_1^2}{2(R_1 + R)h}. \quad (4)$$

$$Nt_{3-0} = \frac{4\pi\sigma_s\mu_s}{\sqrt{3}}V_0\left(1 + \frac{1}{\mathrm{tg}^2\beta}\right)\times$$
$$\times\left[\frac{R_1^2 - R^2}{2} + R(R_1 - R)\right]\frac{R_2^2 - R_1^2}{2(R_1 + R)h}. \quad (5)$$

However, the power of the deformation forces in module 3 is not expressed by elementary functions and requires the use of approximate upper estimates. We find the auxiliary values for the upper estimate of this magnitude:

$$M = \frac{1}{V_0}\iiint_V \dot{\varepsilon}_i^2 dV =$$
$$= \frac{2\pi C^2}{3\mathrm{tg}^3\beta}\left[\left(4\mathrm{tg}^2\beta + \frac{1}{3}\right)\left(R_1 - R + \frac{(R^2 - R_1^2)R}{2R_1^2}\right) - \right.$$
$$\left. -R\ln\frac{R_1}{R} - \frac{(R - R_1)R}{R_1}\right], \quad (6)$$

where

$$C = \frac{R_2^2 - R_1^2}{2h(R_1 + R)}.$$

Thus, we derive an upper estimate of the power of the deformation forces in module 3 by Cauchy-Bunyakovsky:

$$N\partial_3 < \sigma_s V_0\sqrt{VM}, \quad (7)$$

where

$$V=\frac{\pi}{3\mathrm{tg}\beta}\left(2R_1^3+R^3-3R_1^2R\right)$$

– the scope of the module 3 integration region.

Using the upper estimate in the form (7) makes it possible to derive an analytical expression of the reduced deformation pressure in the following form:

$$\bar{p}=\frac{1}{\left(R_2^2-R_1^2\right)}\times$$
$$\times\left[\begin{array}{l}\frac{2}{\sqrt{3}}\left[R_2^2\ln\frac{R_2}{R_1}-\frac{R_2^2-R_1^2}{2}\right]+\\+\frac{2}{\sqrt{3}}\left|\frac{\left(R_2^2-R_1^2\right)\left(3R_1+R\right)}{4R_1\left(R_1^2-R^2\right)}-\alpha\right|+\\+\frac{1}{\sqrt{3}}\left[\frac{2\left(R_2-R_1\right)+}{+\frac{4\left(2\alpha^2-2\alpha+1\right)\left(R_2^3-R_1^3\right)h^2}{3\left(R_2^2-R_1^2\right)^2}}\right]\times\\\times\frac{R_2^2-R_1^2}{h}+\frac{2}{\sqrt{3}}\left[\frac{R_1^2-R^2}{2}+R\left(R_1-R\right)\right]\times\\\times\frac{R_2^2-R_1^2}{2\left(R_1+R\right)h}\left(1+2\mu_s\left(1+\frac{1}{\mathrm{tg}^2\beta}\right)\right)+\\+\frac{4\mu_s}{\sqrt{3}}\frac{\left(R_2^2-R_1^2\right)\left(R+R_1\right)l}{R_1^2-R^2}+\\+\frac{2\mu_s}{\sqrt{3}}R_1\left(H_0-\Delta H_x-h\right)+\frac{\sqrt{VM}}{\pi}\end{array}\right],\qquad(8)$$

where H_0 is the initial height of a blank; ΔH_x is the run.

This function could be considered as a function of the variable parameter $\alpha\in(0,1)$, responsible for the shape of the kinematic module 2 borders, as well as the technological parameters R, R_1, R_2, h of the estimation scheme.

4. 2. Analysis of the magnitude of the reduced pressure of the combined radial-direct extrusion process with compression

By proceeding to the dimensionless magnitudes relative to R_2, we analyze the behavior of the reduced pressure depending on the $\alpha\in(0,h)$ parameter. We use a comparative analysis of the magnitude of the reduced pressure, obtained in the course of numerical integration in the form $\bar{p}_t$, and using the upper estimate in the form $\bar{p}$ given by (8). In this case, the process parameters correspond to the stage of deformation with the complete filling of the metal reversal zone in triangular module 3 (Fig. 2). The character of curves $\bar{p}_t$ (solid line) and upper estimate $\bar{p}$ (dotted line) is identical for different values $\bar{h}=h/R_2$, while the deviation of the upper estimate in the form (8) from $\bar{p}_t$ does not exceed 0.2–1 %. In addition, for these curves, there is no displacement of the minimum point responsible for the optimal value of the parameter α. Thus, the use of the reduced pressure magnitude in the form $\bar{p}$ according to (8) is justified and greatly facilitates the subsequent analysis of this magnitude. In further analysis, we use the upper estimate $\bar{p}$ as the magnitude of the reduced pressure.

The variable parameter that optimizes the magnitude of the reduced pressure is the $\alpha\in(0,1)$, parameter, responsible for the point $B(R_2,\alpha h)$ position and the shape of the kinematic module 2 boundaries (Fig. 3). The character of the curves at different values $\bar{R}=R/R_2$ is strikingly different in determining the minimum point of the reduced pressure magnitude, which corresponds to the optimal value of the parameter α. This is due to the component of the power of the cutting forces of kinematic modules 2 and 3, changing its sign depending on the ratios of geometric parameters and α. For $\bar{R}=0.3$, the minimum point corresponds to the equality to zero of the power of the cutting forces of kinematic modules 2 and 3; for the rest of the values, this condition is not met. The character of the curves at different values $\bar{R}_1=R_1/R_2$ also significantly depends on the component of the power of the cutting forces of kinematic modules 2 and 3; at $\bar{R}_1=0.8$, the minimum point corresponds to the condition $Nc_{2-3}=0$ (Fig. 4). For the rest of the values $\bar{R}_1$, this condition is not met. In this case, an increase in $\bar{R}_1$ leads to a decrease in the magnitude of the reduced pressure and a shift towards reducing the optimal value of the parameter α.

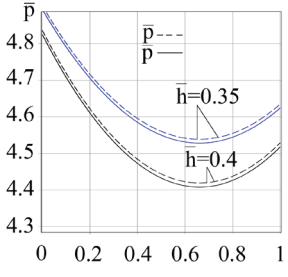

Fig. 2. Dependence of the reduced pressure on parameter α at $\bar{R}=0.3$, $\bar{R}_1=0.5$, $\bar{H}=1$, $\mu_s=0.08$ and different values $\bar{h}$

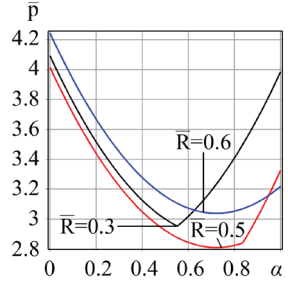

Fig. 3. Dependence of the reduced pressure on parameter α at $\bar{R}_1=0.8$, $\bar{h}=0.5$, $\bar{H}=1$, $\mu_s=0.08$ and different values $\bar{R}$

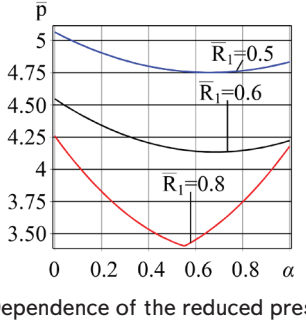

Fig. 4. Dependence of the reduced pressure on parameter α at $\bar{R}=0.3$, $\bar{h}=0.3$, $\bar{H}=1$, $\mu_s=0.08$ and different values $\bar{R}_1$

We shall analytically determine the optimal value of the parameter α, corresponding to the optimal value of the

reduced pressure magnitude, employing the necessary condition of the minimum $\bar{p}'_\alpha = 0$. However, $\bar{p}$ contains an expression of the absolute magnitude that depends on the parameter α, which makes it difficult to find a minimum point and corresponds to the different analytical expressions of the magnitude of reduced pressure, depending on the values in expression (3).

However, for some ratios of the deformation process geometric parameters, an analytical expression could be obtained for the optimal value of the parameter α:

$$\alpha_{opt} = \frac{4R_2^3 + 3R_1R_2^2 - 7R_1^3}{8\left(R_2^3 - R_1^3\right)}$$

at

$$\left(R_2^2 - R_1^2\right)\left(3R_1 + R\right) - 4R_1\left(R_1^2 - R^2\right) > 0. \quad (9)$$

This optimal value corresponds to the curve at $\bar{R} = 0.6$ (Fig. 3) and the curves $\bar{R}_1 = 0.5$ and $\bar{R}_1 = 0.6$ (Fig. 4).

After substituting the optimal value of the parameter α in the formula of the reduced pressure (8), further optimization for geometric parameters is possible, for example, for the angle of inclination of the forming mandrel β (Fig. 5). In order to obtain the components of the required thickness of the extruded wall, the magnitude $\bar{R}$ must be fixed. In this case, the reduction of deformation efforts could be achieved by varying the inclination angle of the forming mandrel β. Reducing the thickness of the extruded wall (an increase in $\bar{R}$) leads to an increase in the magnitude of the reduced pressure and a decrease in the optimal value of the angle of inclination of the forming mandrel. Moreover, for all ratios of geometric parameters, the nature of the curves is identical, the deviation of β from the optimal value towards a decrease leads to a more significant increase in the magnitude of the reduced pressure.

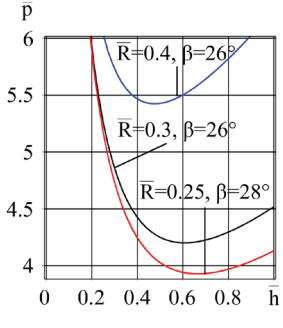

Fig. 5. Dependence of the reduced pressure for $\bar{R}_1 = 0.6$, $\bar{H} = 1.5$, $\bar{H}_x = 0.3$, $\mu_s = 0.1$ at different values of the parameter β

It has been established that among the relative geometric parameters, the magnitude $\bar{p}$ is largely affected by the relative thickness of the extruded wall $\bar{S} = \bar{R}_1 - \bar{R}$ and the inclination angle of the forming mandrel β. With the increase in the magnitude $\bar{R}$, that is with a decrease in the thickness of the extruded wall, the magnitude of reduced pressure increases, which is associated with an increase in the degree of deformation. In this case, the optimal value of the inclination angle of the forming mandrel β decreases; the range of variation of this parameter is within 20° to 30° for different ratios of the deformation process.

5. Comparative analysis of theoretical and experimental data on the force mode of the combined radial-direct extrusion process with compression

In order to verify the adequacy of the acquired estimation data, experimental studies were conducted on the extrusion of hollow components by the combined radial-direct extrusion with compression (Fig. 6, *a*). Components from lead alloy and AA1135 were extruded. A distortion in the dividing grid in zone 2 of the turn in the direct and radial extrusion confirms the validity of the choice of the configuration of kinematic module 2 (Fig. 6, *b*). The study of the stressed-strained state based on FEM and experimental data on the force mode of the radial-direct extrusion process with compression is given in detail in work [9].

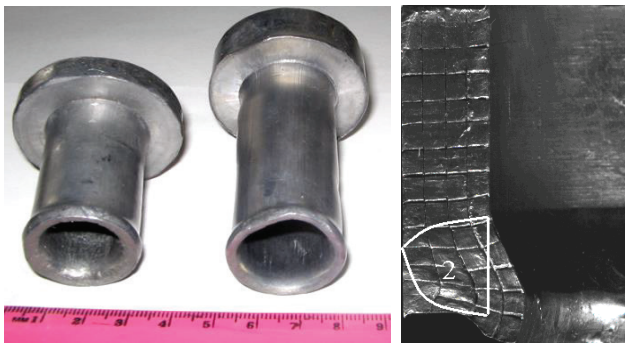

a *b*

Fig. 6. Components obtained by combined radial-direct extrusion with compression: *a* — extruded samples from the AA1135; *b* — distortion of the dividing grid

Based on the results of our study, a chart was built demonstrating the dependence of the extrusion pressure on the course of the press slider at $R_2 = 22.5$ mm, $R_1 = 14$ mm, $h = 11.5$ mm, $H_0 = 30$ mm for the lead alloy blank (Fig. 7). Analysis of the experimentally acquired data (Fig. 7, point data) makes it possible to highlight three stages of the process during extrusion. In the first stage (I), there is a radial flow of the metal until it contacts the mandrel, and then the reversal of the metal and the onset of a direct flow. The flow of the metal is non-stationary and there is an increase in extrusion pressure. In the second stage (II), the flow of the metal is steady, and the extrusion pressure decreases slightly (the decrease is 5–10 %). The decrease in extrusion pressure is explained by a decrease in the area of the friction surface between the workpiece and the tool. In the final stage of the process (III), the deforming punch comes to the deformation site, giving rise to an increase in the pressure of extrusion. At the pressure-motion curve (Fig. 7, point data) this stage appears as an increase in extrusion pressure.

For these deformation process parameters, we derived, based on (9), the optimal value of the variable parameter α_{opt}. Next, based on the analytical expression of the reduced deformation pressure in the form (8) and for $\sigma_s = 22.258 \cdot e^{0.189}$ MPa we derived the dependence of extrusion pressure on the course of the press slider. The deviation in data acquired from the proposed process calculation scheme (Fig. 7, solid line) from the experimentally obtained data does not exceed 13–15 %. In this case, the theoretical calculation corresponds to the slider's run of up to 18 mm up to the degeneration of module 1.

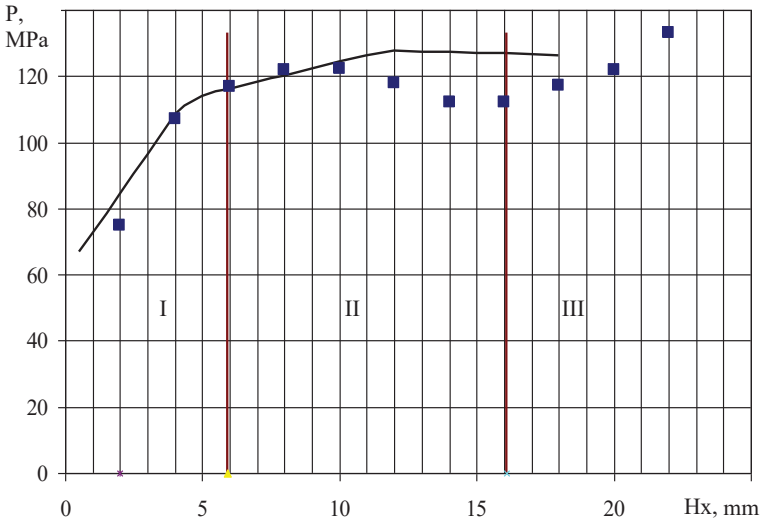

Fig. 7. Dependence chart of extrusion pressure on the press slider run: a theoretical curve (solid line); experiment data (points)

Thus, the developed calculation scheme of the process of combined sequential radial-direct extrusion with compression could be used up to the degeneration of module 1, which corresponds to the slider run equal to H_0–h.

6. Discussion of results of studying the force mode of the combined radial-direct extrusion process with compression

The use of triangular kinematic modules with curvilinear and straight-line boundaries has made it possible to describe the sites of intense deformation for the steady stage of the deformation process. Applying the upper estimate of the power of the deformation forces of kinematic module 3 of the triangular shape has made it possible to derive the magnitude of the reduced deformation pressure in the analytical form (7). Thus, we have solved the problem of calculating the reduced pressure of the new kinematic modules of the triangular shape of type 2 and 3 with different types of boundaries with the complexity of the shape of the deformation sites and the tool geometry. The resulting optimal value of parameter α (9) has made it possible to analyze a change in the magnitude of the reduced deformation pressure (8) at different ratios of the process geometric parameters. It has been established that the optimal inclination angle values of the forming mandrel β lie between 20° and 30° for different ratios of the deformation process (Fig. 5). In this case, the developed calculation scheme of the combined radial-direct extrusion process with compression could also be used for a fixed configuration of the mandrel at the slider's run of up to H_0–h, which is a constraint on the use of the proposed estimation scheme.

To test the validity of the constructed mathematical model of the process, experimental studies were conducted on the extrusion of hollow components from lead alloy and AA1135 by the radial-direct extrusion with compression. The distortion of the dividing grid in zone 2 of the reversal of the direct and radial extrusion confirms the validity of the choice of the configuration of kinematic module 2 (Fig. 6, *b*). In the comparative analysis of the theoretically and experimentally acquired data on the force regime, the effectiveness of the developed calculation scheme of the process (Fig. 7) has been confirmed. In this case, the deviation of data obtained based on the proposed calculation scheme of the process from those experimentally acquired does not exceed 13–15 %.

Note that the power of deformation forces in the form (7) and the power of friction forces in the form (5) for kinematic module 3 could be used in various calculation schemes when changing the neighboring kinematic modules. Adjustments would be required only for the calculation of the power of the cutting forces.

It is promising to further develop the new curvilinear kinematic modules of different configurations, to advance the simplification techniques to calculate them and to study their integration into more complex estimation schemes of the combined extrusion processes.

7. Conclusions

1. The estimation scheme of the process of combined radial-direct extrusion with compression using triangular modules with curvilinear and rectilinear boundaries has been built. This has made it possible to derive an analytical expression of the reduced pressure at the slider's run of up to H_0–h.

2. The effect of the tool geometry on the force mode of the combined radial-direct extrusion process with compression has been investigated. It has been established that the magnitude of the reduced pressure is most influenced by the relative thickness of the extruded wall $\overline{S} = \overline{R_1} - \overline{R}$ and the angle of inclination of the forming mandrel β. With decreasing thickness of the extruded wall, the magnitude of the reduced pressure increases, which is associated with an increase in the degree of deformation. In this case, the optimal value of the angle of inclination of the forming mandrel β decreases and is in the range from 20° to 30° for various ratios of the deformation process.

3. Experimental studies on the distortion of the dividing grid confirm the rationality of the choice of the configuration of kinematic module 2 of a triangular shape with curvilinear borders. A comparative analysis of force regimes obtained theoretically and experimentally also confirms the viability of the developed estimation process scheme. The deviation of the data obtained on the basis of the proposed calculation scheme of the process from the experimentally obtained data on extrusion pressure does not exceed 13–15 %.

References

1. Bhaduri, A. (2018). Extrusion. Springer Series in Materials Science, 599–646. doi: https://doi.org/10.1007/978-981-10-7209-3_13
2. Aliiev, I. S. (1988). Radial extrusion processes. Soviet Forging and Sheet Metal Stamping Technology, 6, 1–4.
3. Saffar, S., Malaki, M., Mollaei-Dariani, B. (2014). On the effects of eccentricity in precision forging process. UPB Scientific Bulletin, Series D: Mechanical Engineering, 76 (1), 123–138.

4. Aliiev, I. S., Lobanov, A. I., Borisov, R. S., Savchinskij, I. G. (2004). Investigation of die blocks with split matrixes for the processes of cross extrusion. Kuznechno-Shtampovochnoe Proizvodstvo (Obrabotka Metallov Davleniem), 8, 21–26.
5. Aliieva, L. I. (2016). Protsessy kombinirovannogo plasticheskogo deformirovaniya i vydavlivaniya. Obrabotka materialov davleniem, 1, 100–108.
6. Kalyuzhnyi, V. L., Alieva, L. I., Kartamyshev, D. A., Savchinskii, I. G. (2017). Simulation of Cold Extrusion of Hollow Parts. Metallurgist, 61 (5-6), 359–365. doi: https://doi.org/10.1007/s11015-017-0501-1
7. Jafarzadeh, H., Zadshakoyan, M., Abdi Sobbouhi, E. (2010). Numerical Studies of Some Important Design Factors in Radial-Forward Extrusion Process. Materials and Manufacturing Processes, 25 (8), 857–863. doi: https://doi.org/10.1080/10426910903536741
8. Xue, Y., Bai, B., Chen, S., Li, H., Zhang, Z., Yang, B. (2017). Study on processing and structure property of Al-Cu-Mg-Zn alloy cup-shaped part produced by radial-backward extrusion. The International Journal of Advanced Manufacturing Technology, 95 (1-4), 687–696. doi: https://doi.org/10.1007/s00170-017-1073-8
9. Shatermashhadi, V., Manafi, B., Abrinia, K., Faraji, G., Sanei, M. (2014). Development of a novel method for the backward extrusion. Materials & Design (1980-2015), 62, 361–366. doi: https://doi.org/10.1016/j.matdes.2014.05.022
10. Aliieva, L., Zhbankov, Y. (2015). Radial-direct extrusion with a movable mandrel. Metallurgical and Mining Industry, 11, 175–183.
11. Farhoumand, A., Khoddam, S., Hodgson, P. D. (2012). A study of plastic deformation during axisymmetric forward spiral extrusion and its subsequent mechanical property changes. Modelling and Simulation in Materials Science and Engineering, 20 (8), 085005. doi: https://doi.org/10.1088/0965-0393/20/8/085005
12. Murata, M., Kuboki, T., Kobayashi, M., Yamazaki, H. (2012). Influence of Billet Material of Extruded Circular Tube with Spiral Projections on Inside Wall. Influence of billet material of extruded circular tube with spiral projections on inside wall, Metal forming. Krakow, 463–466.
13. Noh, J., Hwang, B. B., Lee, H. Y. (2015). Influence of punch face angle and reduction on flow mode in backward and combined radial backward extrusion process. Metals and Materials International, 21 (6), 1091–1100. doi: https://doi.org/10.1007/s12540-015-5276-y
14. Jamali, S. S., Faraji, G., Abrinia, K. (2016). Hydrostatic radial forward tube extrusion as a new plastic deformation method for producing seamless tubes. The International Journal of Advanced Manufacturing Technology, 88 (1-4), 291–301. doi: https://doi.org/10.1007/s00170-016-8754-6
15. Ogorodnikov, V. A., Dereven'ko, I. A., Sivak, R. I. (2018). On the Influence of Curvature of the Trajectories of Deformation of a Volume of the Material by Pressing on Its Plasticity Under the Conditions of Complex Loading. Materials Science, 54 (3), 326–332. doi: https://doi.org/10.1007/s11003-018-0188-x
16. Noh, J., Hwang, B.-B. (2015). Numerical analysis of tool geometry effect on the wear characteristics in a radial forward extrusion. Journal of Mechanical Science and Technology, 29 (8), 3447–3457. doi: https://doi.org/10.1007/s12206-015-0743-4
17. Farhoumand, A., Ebrahimi, R. (2016). Experimental investigation and numerical simulation of plastic flow behavior during forward-backward-radial extrusion process. Progress in Natural Science: Materials International, 26 (6), 650–656. doi: https://doi.org/10.1016/j.pnsc.2016.12.005
18. Aliiev, I., Aliieva, L., Grudkina, N., Zhbankov, I. (2011). Prediction of the Variation of the Form in the Processes of Extrusion. Metallurgical and Mining Industry, 3 (7), 17–22.
19. Motallebi Savarabadi, M., Faraji, G., Zalnezhad, E. (2019). Hydrostatic tube cyclic expansion extrusion (HTCEE) as a new severe plastic deformation method for producing long nanostructured tubes. Journal of Alloys and Compounds, 785, 163–168. doi: https://doi.org/10.1016/j.jallcom.2019.01.149
20. Ebrahimi, R., Reihanian, M., Moshksar, M. M. (2008). An analytical approach for radial-forward extrusion process. Materials and Design, 29, 1694–1700.
21. Noh, J. H., Hwang, B. B. (2017). Work efficiency in a double cup extrusion process. International Journal of Precision Engineering and Manufacturing, 18 (3), 407–414. doi: https://doi.org/10.1007/s12541-017-0049-9
22. Alyushin, Yu. A. (2012). Mehanika tverdogo tela v peremennyh Lagranzha. Moscow: Mashinostroenie, 192.
23. Chudakov, P. D. (1992). Verhnyaya otsenka moshchnosti plasticheskoy deformatsii s ispol'zovaniem minimiziruyushchey funktsii. Izvestiya vuzov. Mashinostroenie, 9, 13–15.
24. Unksov, E. P., Dzhonson, U., Kolmogorov, V. L., Ogorodnikov, V. A. et. al.; Unksov, E. P., Ovchinnikov, A. G. (Eds.) (1992). Teoriya kovki i shtampovki. Moscow: Mashinostroenie, 720.
25. Hrudkina, N., Aliieva, L., Abhari, P., Kuznetsov, M., Shevtsov, S. (2019). Derivation of engineering formulas in order to calculate energy-power parameters and a shape change in a semi-finished product in the process of combined extrusion. Eastern-European Journal of Enterprise Technologies, 2 (7 (98)), 49–57. doi: https://doi.org/10.15587/1729-4061.2019.160585
26. Hrudkina, N., Aliieva, L., Abhari, P., Markov, O., Sukhovirska, L. (2019). Investigating the process of shrinkage depression formation at the combined radial-backward extrusion of parts with a flange. Eastern-European Journal of Enterprise Technologies, 5 (1 (101)), 49–57. doi: https://doi.org/10.15587/1729-4061.2019.179232
27. Vlasenko, K., Hrudkina, N., Reutova, I., Chumak, O. (2018). Development of calculation schemes for the combined extrusion to predict the shape formation of axisymmetric parts with a flange. Eastern-European Journal of Enterprise Technologies, 3 (1 (93)), 51–59. doi: https://doi.org/10.15587/1729-4061.2018.131766